NATIONAL ADVISORY COMMITTEE FOR AERONAUTICS

TECHNICAL NOTE 2561

A STUDY OF POISSON'S RATIO IN THE YIELD REGION

By George Gerard and Sorrel Wildhorn

New York University

Washington

January 1952

NATIONAL ADVISORY COMMITTEE FOR AERONAUTICS

TECHNICAL NOTE 2561

A STUDY OF POISSON'S RATIO IN THE YIELD REGION

By George Gerard and Sorrel Wildhorn

SUMMARY

In the yield region of the stress-strain curve the variation in Poisson's ratio from the elastic to the plastic value is most pronounced. This variation was studied experimentally by a systematic series of tests on several aluminum alloys. The tests were conducted under simple tensile and compressive loading along three orthogonal axes.

A theoretical variation of Poisson's ratio for an orthotropic solid was obtained from dilatational considerations. The assumptions used in deriving the theory were examined by use of the test data and were found to be in reasonable agreement with experimental evidence.

INTRODUCTION

Poisson's ratio for engineering materials under simple axial loading usually has a value in the elastic region of between 1/4 and 1/3 and on the assumption of a plastically incompressible isotropic solid assumes a value of 1/2 in the plastic region. The transition from the elastic to the plastic value, in general, is gradual and is most pronounced in the yield region of the stress-strain curve.

In the deformation theory of small elastic and plastic strains for an isotropic solid, which is summarized by Nadai in reference 1, it is shown that the stress-strain relations for a strain-hardening material depend essentially upon two deformation functions, the secant modulus and the generalized Poisson's ratio. Because of the fundamental nature of the latter in any plasticity theory, this investigation was undertaken to provide basic experimental data on the variation of Poisson's ratio in the yield region of some materials commonly employed in aircraft applications.

General dilatational relations are considered in the section entitled "Theoretical Investigation" and it is found that a theoretical relationship for the variation of Poisson's ratio from the elastic to the plastic value can be obtained for an orthotropic medium in which the plane containing the two isotropic axes is normal to the applied load. This

relationship depends upon the elastic value of Poisson's ratio, the shape of the stress-strain curve as given by the ratio of the secant to the elastic modulus, and a plastic value of Poisson's ratio.

Systematic experimental studies of the variation of Poisson's ratio in the yield region are generally lacking in the literature. One study is a report by Stang, Greenspan, and Newman (reference 2) for aluminum alloys and low-carbon steels. Values of Poisson's ratio under simple tensile loading were obtained for strains as high as 18 percent on thin flat tensile specimens.

It appears that a completely systematic series of tests should include both tensile and compressive stress-strain properties along three orthogonal axes as well as the Poisson ratio variation along these directions under simple tensile and compressive loadings. An investigation of this type was carried out for three commonly used aluminum alloys: Rolled 24S-T4 and extruded 14S-T6 and 75S-T6. The results are given in the section entitled "Experimental Investigation."

In the section entitled "Correlation of Theory and Test Data" the validity of the theoretical relationship for the variation of Poisson's ratio is examined by comparison with the experimental results.

This investigation was conducted under the sponsorship and with the financial assistance of the National Advisory Committee for Aeronautics. The authors wish to acknowledge their indebtedness to Mr. Gary Gould for valuable assistance in the experimental investigation and Mr. Conrad Schmidt for machining of the test specimens.

SYMBOLS

E	modulus of elasticity
$\overline{E}$	secant modulus
I	quadratic strain invariant; defined in equation (6)
σ	normal stress
τ	shear stress
ϵ	normal strain $\left(\sigma/\overline{E}\right)$
γ	shear strain
ν	generalized Poisson's ratio $\left(-\epsilon_y/\epsilon_x\right)$

ϵ^*	elastic strain (σ/E)
δ	strain deviation $(\epsilon - \epsilon^*)$
ϑ	cubical dilatation
μ	variation of Poisson's ratio from elastic value $(\nu - \nu^*)$
x,y,z	Cartesian coordinates

Superscripts:

*	elastic component
—	plastic component

Where two subscripts are used, the first refers to the direction in which the load is applied and the second to the reference direction.

THEORETICAL CONSIDERATIONS

Transforms of Simple Tension to Simple Shear

For the purpose of indicating the magnitude of the effect of the Poisson ratio variation in a simple case, it is instructive to consider the derivation of the affinity terms which transform a simple tensile stress-strain curve into a simple shear stress-strain curve. Since Poisson's ratio is associated with strain only, the stress transformations are written immediately.

According to the maximum-shear theory

$$\tau = 0.5\sigma \tag{1}$$

For the octahedral-shear theory

$$\tau = \sigma/\sqrt{3} \tag{2}$$

The maximum-shear theory states that

$$\gamma = \epsilon_x - \epsilon_y \tag{3}$$

In simple tension, $\epsilon_y = -\nu\epsilon$ and thus from equation (3)

$$\gamma = (1 + \nu)\epsilon \tag{4}$$

The octahedral shear strain can be written in the following form:

$$\gamma_{oct} = \sqrt{8I/3} \tag{5}$$

where I is the quadratic strain invariant,

$$I = \frac{1}{2}\left(\epsilon_x^2 + \epsilon_y^2 + \epsilon_z^2\right) + \frac{1}{4}\left(\gamma_{xy}^2 + \gamma_{yz}^2 + \gamma_{zx}^2\right) \tag{6}$$

In simple tension

$$\gamma_{oct} = \epsilon\sqrt{4\left(1 + 2\nu^2\right)/3} \tag{7}$$

In simple shear

$$\gamma_{oct} = \gamma\sqrt{2/3} \tag{8}$$

The affinity relationship is obtained by equating equations (7) and (8)

$$\gamma = \epsilon\sqrt{2\left(1 + 2\nu^2\right)} \tag{9}$$

Thus, from equations (4) and (9), it is evident that the strain affinity terms are actually functions of Poisson's ratio. The limiting values which the affinity terms can assume for a plastically incompressible solid are given in the following table for typical values of Poisson's ratio:

Theory	Affinity term	Lower limit $\nu^* = 0.3$	Upper limit $\bar{\nu} = 0.5$
Maximum shear	$(1 + \nu)$	1.3	1.5
Octahedral shear	$\sqrt{2\left(1 + 2\nu^2\right)}$	1.53	$\sqrt{3}$

Theoretical Poisson Ratio Variation

The cubical dilatation of a strained solid is given by

$$\vartheta = \epsilon_x + \epsilon_y + \epsilon_z + \epsilon_x\epsilon_y + \epsilon_y\epsilon_z + \epsilon_z\epsilon_x + \epsilon_x\epsilon_y\epsilon_z \tag{10}$$

If infinitesimal strains are considered, which is a reasonable assumption in the yield region, the second- and third-order terms of the dilatation may be neglected. In so doing, the dilatation is equal to the linear strain invariant:

$$\vartheta = \epsilon_x + \epsilon_y + \epsilon_z \tag{11}$$

The behavior of engineering materials indicates that the total strain can be considered to be composed of two parts: The elastic strain component ϵ^* and the strain deviation δ. Thus, the dilatation can be written

$$\vartheta = \left(\epsilon_x^* + \epsilon_y^* + \epsilon_z^*\right) + \left(\delta_x + \delta_y + \delta_z\right) \tag{12}$$

By considering the dilatation to be composed of elastic and plastic components,

$$\vartheta = \vartheta^* + \overline{\vartheta} \tag{13}$$

where

$$\vartheta^* = \epsilon_x^* + \epsilon_y^* + \epsilon_z^* \tag{14}$$

$$\overline{\vartheta} = \delta_x + \delta_y + \delta_z \tag{15}$$

The usual assumption of mathematical plasticity theory that the dilatation vanishes is obtained by neglecting the elastic component and assuming that the plastic component is zero.

Consider a solid subjected to a simple tensile load in the x-direction. Upon making the assumption that the solid is isotropic along the other two orthogonal axes, the various dilatations can be determined. Such a solid is referred to as orthotropic.

For the elastic component, from equation (14)

$$\vartheta^* = \epsilon^*(1 - 2\nu^*) \tag{16}$$

and for the plastic component it is assumed that for the orthotropic solid equation (15) can be written as

$$\overline{\vartheta} = \delta(1 - 2\overline{\nu}) \tag{17}$$

The total dilatation, from equation (13) is

$$\vartheta = \epsilon^*(1 - 2\nu^*) + \delta(1 - 2\overline{\nu}) \tag{18}$$

It is further assumed that for an orthotropic solid the total dilatation can be referred to the total strain by the relation

$$\vartheta = \epsilon(1 - 2\nu) \tag{19}$$

Combining equations (18) and (19) and simplifying, the variation of Poisson's ratio as a function of strain is given by

$$\nu = \overline{\nu} - \frac{\epsilon^*}{\epsilon}(\overline{\nu} - \nu^*) \tag{20}$$

For cases in which the plastic dilatation vanishes, $\overline{\vartheta} = 0$, and from equation (17), $\overline{\nu} = 0.5$. In this special case, equation (20) reduces to

$$\nu = 0.5 - \frac{\epsilon^*}{\epsilon}(0.5 - \nu^*)$$

or

$$\nu = 0.5 - \frac{\overline{E}}{E}(0.5 - \nu^*) \tag{20a}$$

When unloading follows loading into the plastic range, equations (20) and (20a) yield the elastic value of Poisson's ratio since the term ϵ^*/ϵ then becomes equal to unity.

An expression for the generalized Poisson's ratio which corresponds to equation (20a) is also given by Nádai in reference 1.

EXPERIMENTAL INVESTIGATION

Description of Test Specimens

The materials under investigation were loaded in tension and compression along each direction of a set of three orthogonal axes x, y, and z where the z-direction is the direction of extrusion or rolling. The materials tested were rolled 24S-T4 aluminum alloy and extruded 14S-T6 and 75S-T6 aluminum alloy. The specimens were cut from bars of square cross section with sides equal to $3\frac{1}{4}$ inches.

Engineering materials generally lack isotropy and, in addition, the properties may vary from point to point in the cross section. Therefore, the specimens were cut from each bar in such a manner that strain measurements were taken at essentially the same location in all tests.

A drawing of the tension and compression specimens is shown in figure 1. The tension specimens were loaded through special grips designed for this investigation. The grips were seated in spherical bearings to insure application of axial loading to the specimen and are shown with a specimen installed in figure 2.

The compression specimens were machined flat, square, and parallel and carefully placed in the testing machine to minimize bending.

Test Procedure

Load was applied to the specimens by a Baldwin-Southwark universal hydraulic testing machine of 200,000-pound capacity with an accuracy of loading of ±1/2 percent. AX-5 strain gages were mounted on each of the four sides of each specimen. A wired tension specimen is shown in figure 3.

Strains were measured with a Baldwin SR-4 strain indicator. The estimated accuracy of the strain measurements is approximately ±2 percent. The errors in the strain measurements are associated with the strain indicator, the stated gage factor of the strain gage, and slight drift of the strain readings at large plastic strains.

Experimental Results

A complete set of stress-strain curves for each of the aluminum alloys tested is given in figures 4, 5, and 6. Poisson's ratio in the yield region is given in figures 7 to 12 for both tension and compression with the load applied along each of the three coordinate axes. Poisson's ratio was computed by taking the negative of the ratio of corrected transverse strain to strain in the direction of loading. Corrections for the measured transverse strains are necessary because of the construction of the wire resistance strain gage. The method of correction is given in the appendix.

A quantity of considerable interest in the theoretical study was the nature of the plastic dilatation. Accordingly, the plastic dilatation as a function of strain deviation is given in figures 13, 14, and 15 for the materials studied. The strain deviations were computed according to the definition of this quantity, and the plastic dilatation was obtained by equation (15).

Discussion of Experimental Results

In all cases, the values of strain shown in the figures were obtained by averaging each back-to-back set of strain gages to eliminate any bending. In the worst case, it was found that the maximum bending strain was approximately 4 percent of the axial strain.

In several of the plots of Poisson's ratio variation shown in figures 7 to 12 it can be observed that the elastic value of Poisson's ratio is not constant. Any scatter which exists at the first few loading points may possibly be attributed to experimental technique. However, the consistent variation of the elastic Poisson's ratio shown for the tension specimens in figure 10 suggests that a nonconstant elastic Poisson's ratio may actually be a property of the materials tested. That such behavior was not observed in reference 2, and possibly in other investigations, is attributed to the fact that the elastic Poisson's ratio was computed as the ratio of the slopes of straight lines drawn through stress-axial-strain and stress-transverse-strain data in the elastic region.

CORRELATION OF THEORY AND TEST DATA

A significant feature of the experimental study is contained in figures 13, 14, and 15 which show that the plastic dilatation is not zero for the aluminum alloys under investigation. This experimental fact may be attributed, in part, to the anisotropic character of these engineering materials.

The theoretical variation of Poisson's ratio given in the section entitled "Theoretical Consideration" was derived for an orthotropic solid. The stress-strain characteristics of the alloys used for the experimental investigation indicate that the cases given in the following table may be considered orthotropic if it is assumed that the transverse strains are induced by an effective transverse load of the same sense as the applied load.

Material	Loading
14S-T6	Tension in z-direction
24S-T4	Tension in z-direction
24S-T4	Compression in z-direction
75S-T6	Tension in z-direction

Thus, experimental data are provided for examination of the theoretical variation of Poisson's ratio given in "Theoretical Considerations" by the relation

$$\nu = \bar{\nu} - \frac{\epsilon^*}{\epsilon}(\bar{\nu} - \nu^*) \tag{20}$$

Poisson's ratio for various plastic strains may be computed by use of equation (20) if the following quantities are known:

(a) The elastic value of Poisson's ratio ν^*

(b) The stress-strain characteristics of the material in the direction of application of load from which ϵ^*/ϵ can be computed

(c) The term $\bar{\nu}$ which for a plastically incompressible isotropic solid has the constant value of 1/2

The coefficient $\bar{\nu}$ bears further discussion since it is a term which apparently incorporates the effects of nonvanishing plastic dilatation. From equation (20) this coefficient may be expressed as

$$\lim_{\epsilon^*/\epsilon \to 0} \nu = \bar{\nu} \tag{21}$$

It is the asymtotic value of the Poisson ratio variation to which the elastic properties make no contribution, or it can be imagined as the strain ratio of a material in which the dilatations were purely plastic. It is referred to hereafter as the asymptotic strain ratio.

Furthermore, the plastic dilatation for an orthotropic material was assumed to be given by

$$\bar{\vartheta} = \delta(1 - 2\bar{\nu}) \tag{17}$$

If the asymptotic strain ratio is a constant, then the plastic dilatation should be a linear function of the strain deviation.

An examination of figures 13, 14, and 15 for the orthotropic cases listed in the preceding table indicated that although considerable scatter does exist among the experimental points, a possible linear relationship exists between plastic dilatation and strain deviation within the range of strains considered. A straight line was passed through the test data by the method of least squares and $\bar{\nu}$ was computed from

$$\bar{\nu} = \frac{1}{2}\left(1 - \frac{\bar{\vartheta}}{\delta}\right) \tag{17a}$$

The values of $\bar{\nu}$ obtained from figures 13, 14, and 15 by means of equation (17a) are given in the following table:

Material	Loading	Computed $\bar{\nu}$	$\bar{\nu} - \nu^*$
14S-T6	Tension in z-direction	0.65	0.30
24S-T4	Tension in z-direction	.56	.22
24S-T4	Compression in z-direction	.63	.29
75S-T6	Tension in z-direction	.60	.25

To test further the validity of the theory by use of the experimental data contained herein, it is proposed to examine these data by use of equation (20) to determine if the value of the asymptotic strain ratio is constant for various strains and compares with the values given in the preceding table. For this purpose, equation (20) can be rewritten in the form

$$\bar{\nu} = \frac{\nu - \nu^* \frac{\epsilon^*}{\epsilon}}{1 - \frac{\epsilon^*}{\epsilon}} \tag{22}$$

Equation (22) can be simplified by letting

$$\nu = \nu^* + \mu \tag{23}$$

where μ is the change in ν from the elastic value. With this substitution, equation (22) reduces to

$$\bar{\nu} - \nu^* = \frac{\mu}{1 - \frac{\epsilon^*}{\epsilon}} \tag{24}$$

For the cases listed in the table above, values of μ as a function of ϵ were obtained from curves faired through the test data given in figures 7, 9, and 11. The values of ϵ^*/ϵ were computed from the stress-strain curves of the materials given in figures 4, 5, and 6. Then by use of equation (24) the asymptotic strain ratios were calculated for the

series of selected points. These data are shown in figure 16 as compared with the values of the asymptotic strain ratio given in the preceding table.

Reasonably good agreement exists between the two methods of computation among all the cases except for 14S-T6 aluminum alloy. The greatest discrepancies between the two sets of data occur at values of ϵ^*/ϵ approaching unity. The nature of equation (24) is such that large errors are associated with this range of ϵ^*/ϵ values and consequently more weight should be given to the points removed from this region.

DISCUSSION

The Poisson's ratio test data presented herein for the yield region of the stress-strain curve exhibit the same general characteristics as the test data given in reference 2 for similar aluminum alloys. The tests reported in reference 2, however, also go far beyond the yield region and indicate that in many cases the variation of Poisson's ratio reaches a maximum at a strain of between 2 and 6 percent and then steadily decreases.

It appears that this behavior can be attributed to the fact that beyond a strain of approximately 2 percent the strains are no longer small in the sense that the second- and third-order terms in the dilatation equation (10) may be neglected. This is demonstrated in reference 2 by computing Poisson's ratio for a plastically incompressible isotropic solid using the following expression which can be derived from equation (10) with the above assumptions:

$$\nu = \frac{1 - \left(\frac{1 + \vartheta}{1 + \epsilon}\right)^{1/2}}{\epsilon} \qquad (25)$$

A comparison of numerical results obtained from equation (25) and the variation of Poisson's ratio given by equation (20) reveals that the latter is adequate up to a strain of approximately 2 percent. Beyond this value of strain, equation (20) asymptotically approaches a maximum, whereas equation (25) reaches a maximum and then decreases in substantial agreement with the experimental behavior observed in reference 2.

The test data on plastic dilatation obtained from strain measurements and shown in figures 13, 14, and 15 indicate that tensile loading in the yield region is accompanied by a permanent decrease in volume, whereas compression results in a permanent increase in volume. These data were subsequently checked by density measurements on several

specimens used in the experimental investigation of Poisson's ratio and also by independent volume measurements on a block of 14S-T6 aluminum alloy compressed in the y-direction to various values of strain deviation. From the latter, the data indicate that the volume changes noted appear to be associated with the yield region only and apparently decrease to negligible volume changes beyond a strain deviation of the order of 0.02 inch per inch.

CONCLUDING REMARKS

A systematic set of test data for the variation of Poisson's ratio in the yield region of the stress-strain curve is presented for the aluminum alloys 14S-T6, 24S-T4, and 75S-T6. The test data are for simple tensile or compressive loading along three orthogonal axes.

For an orthotropic solid, a theoretical variation of Poisson's ratio in the yield region was obtained from dilatational considerations. Certain of the test data indicated that under the loading used the material could be considered orthotropic. These data were used to confirm the validity of the assumptions made in deriving the theoretical variation of Poisson's ratio.

Daniel Guggenheim School of Aeronautics
College of Engineering
New York University
New York, N.Y., November 14, 1950

APPENDIX

GAGE-FACTOR CORRECTION FOR A ONE-DIMENSIONAL STRESS FIELD

The use of 90° crossed-type (×) resistance strain gages in a one-dimensional stress field requires that a correction be applied to the stated gage factor of the gage which is perpendicular to the applied load. This correction arises from the fact that the end loops of the transverse gage are subjected to a different strain from that used to determine the stated gage factor. The stated gage factor of the strain gage alined in the direction of the applied load requires no correction since the manner of loading used in the test corresponds to that used in calibration of the gage.

The symbols used in the following discussion are:

R	resistance of strain-sensitive wire
ρ	resisitivity
L	length of strain-sensitive wire
A	area of strain-sensitive wire
k	constant involving changes in ρ, L, and A
l	length of strain-gage grid
w	width of strain-gage grid
n	number of grip loops plus 1
G	gage factor
r	strain reading

The initial resistance of a strain gage in which the strain-sensitive wire is arranged in the conventional rectangular grid is

$$R_o = \rho_o L_o / A_o \qquad (A1)$$

Under deformation, the resistance is changed by the increment $\Delta(\rho L/A)$ which involves changes in ρ, L, and A. It is known, however, that this increment is a function of the deformation of the wire only. Thus

$$\frac{\Delta R}{R_o} = \frac{kA_o}{\rho_o}\left(\frac{\epsilon_1 n l + \epsilon_2 w}{n l + w}\right) \tag{A2}$$

where ϵ_1 is the strain along the axis of the gage and ϵ_2 is the transverse strain. For loadings in which $\epsilon_1 = -\nu\epsilon_2$, equation (A2) can be rewritten in the form

$$\frac{\Delta R/R_o}{G} = \epsilon_1 + \left(1 - \nu^2\right)\epsilon_2 \frac{w}{n l - \nu w} \tag{A3}$$

where

$$G = \frac{kA_o}{\rho_o}\left(\frac{n l - \nu w}{n l + w}\right)$$

The left-hand term of equation (A3) is the reading obtained from the strain indicator. Equation (A3) can be written approximately as

$$r = \epsilon_1 + \left(1 - \nu^2\right)\epsilon_2 \left(w/n l\right) \tag{A4}$$

The corrected transverse strain is then

$$\epsilon_1 = r - \left(1 - \nu^2\right)\epsilon_2 \left(w/n l\right) \tag{A5}$$

For the AX-5 strain gage used in the test described in the section entitled "Experimental Investigation," $n = 10$ and $w/l = 0.5$. Thus

$$\epsilon_1 = r - 0.05\left(1 - \nu^2\right)\epsilon_2 \tag{A6}$$

The only difficulty encountered in using equation (A6) to correct the transverse strain measurements is that Poisson's ratio was unknown. As a first approximation ν was calculated by taking the negative of r/ϵ_2. It was found that a second approximation was unnecessary.

REFERENCES

1. Nádai, Arpád: Theory of Flow and Fracture of Solids. Vol. I. Second ed., McGraw-Hill Book Co., Inc., 1950, pp. 379-387.

2. Stang, Ambrose H., Greenspan, Martin, and Newman, Sanford B.: Poisson's Ratio of Some Structural Alloys for Large Strains. Res. Paper RP 1742, Jour. Res., Nat. Bur. of Standards, vol. 37, no. 4, Oct. 1946, pp. 211-221.

Tension specimen

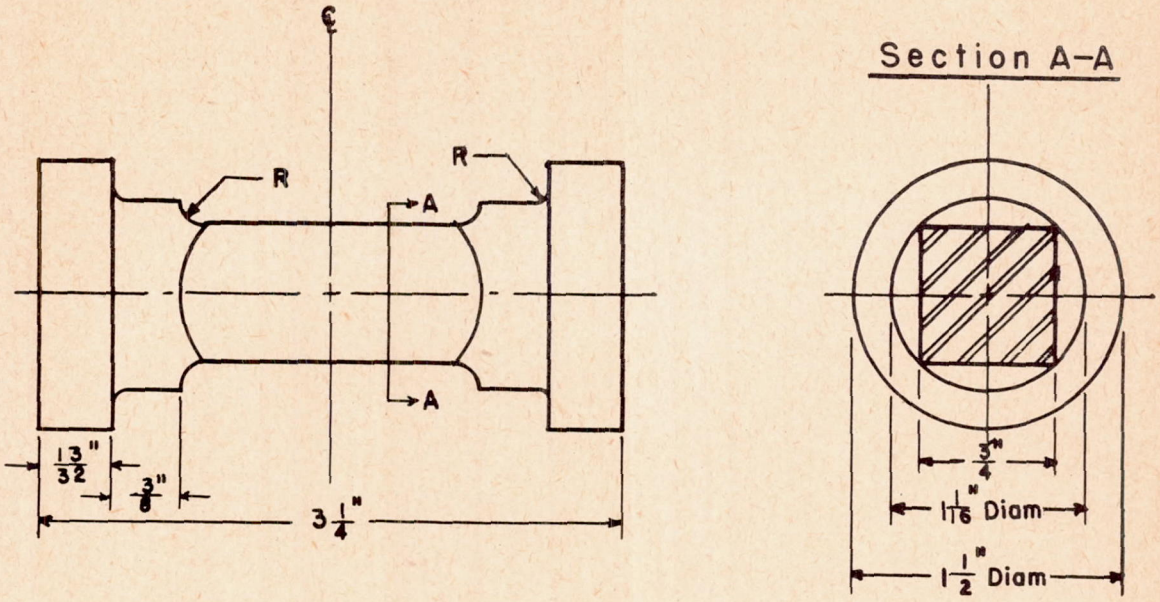

Compression specimen

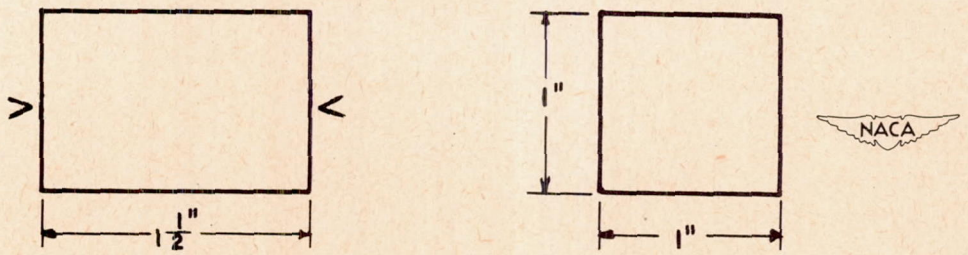

Figure 1.- Tension and compression specimens used in experimental investigation. V-ends are to be flat, square, and parallel within ±0.002 inch.

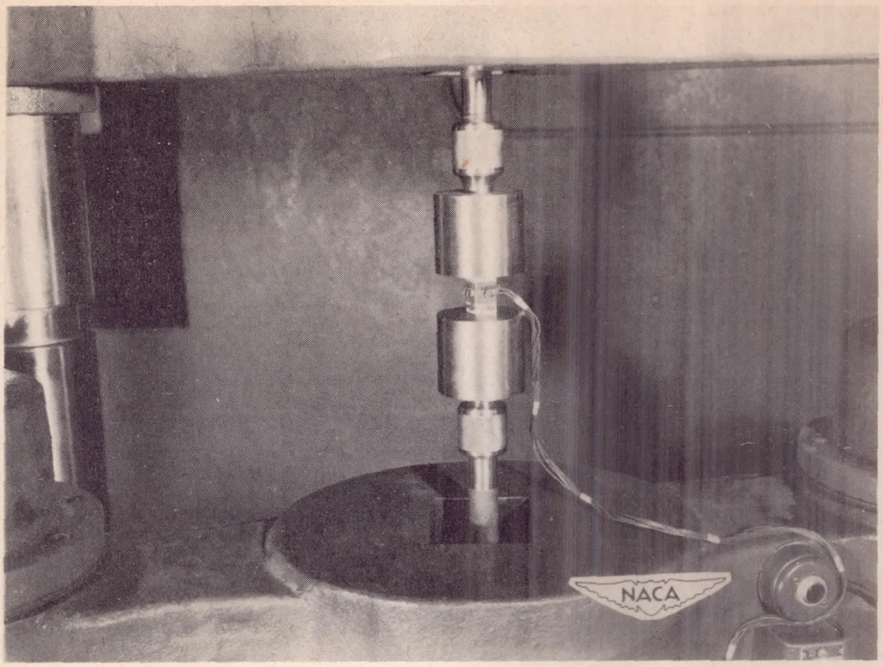

Figure 2.- Tension specimen in testing machine.

Figure 3.- Wired tension specimen.

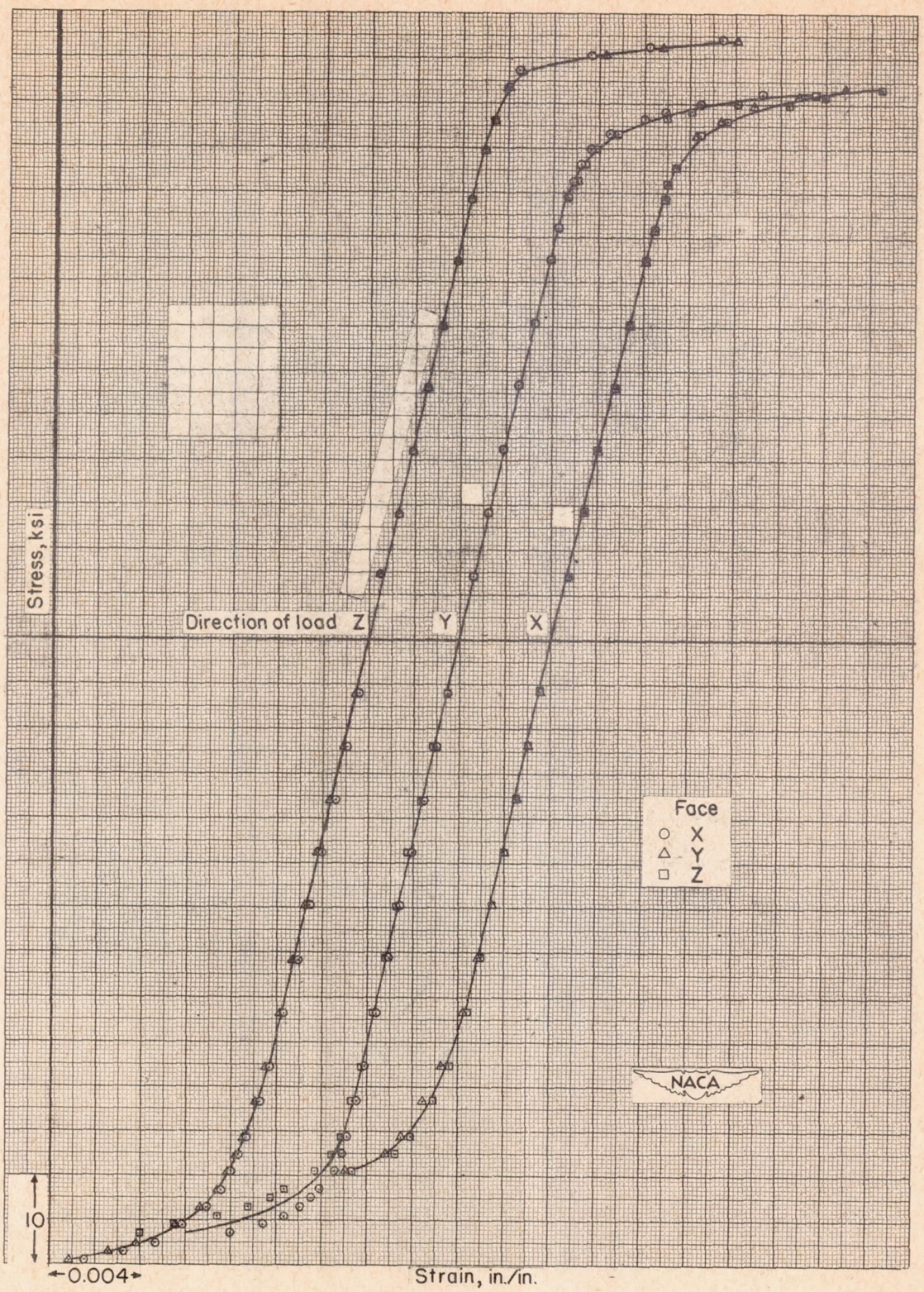

Figure 4.- Stress-strain curves for 14S-T6 aluminum alloy.

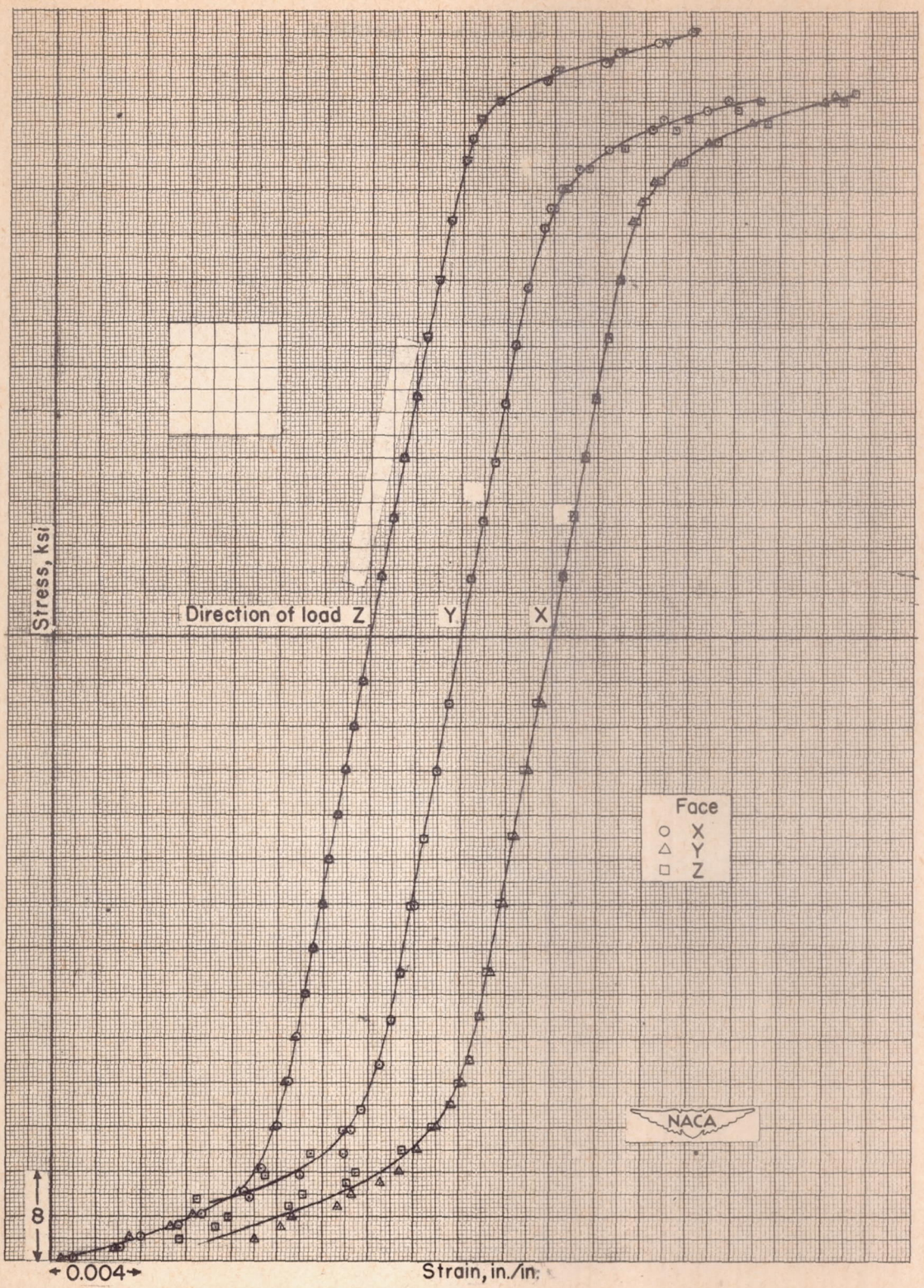

Figure 5.- Stress-strain curves for 24S-T4 aluminum alloy.

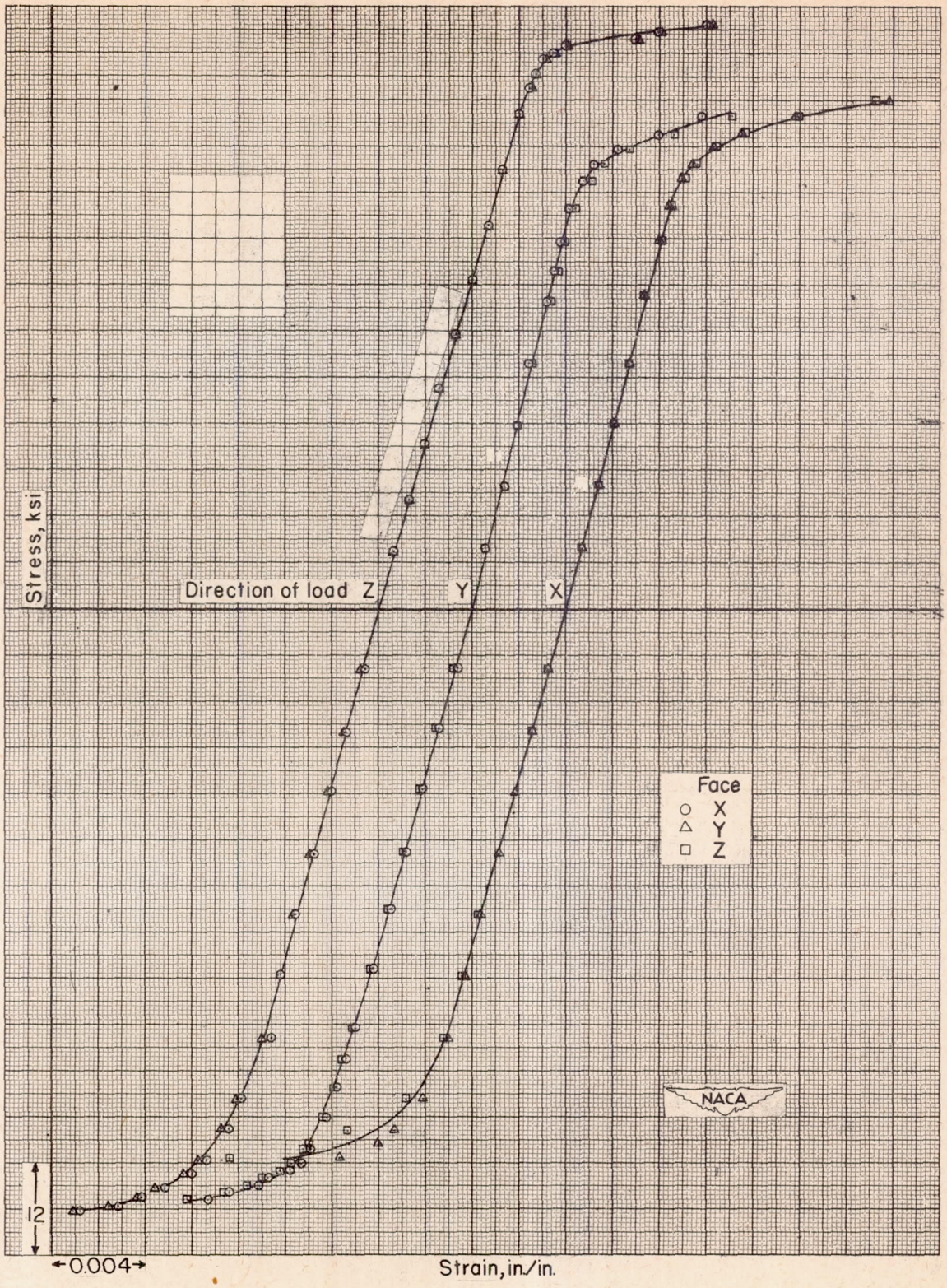

Figure 6.- Stress-strain curves for 75S-T6 aluminum alloy.

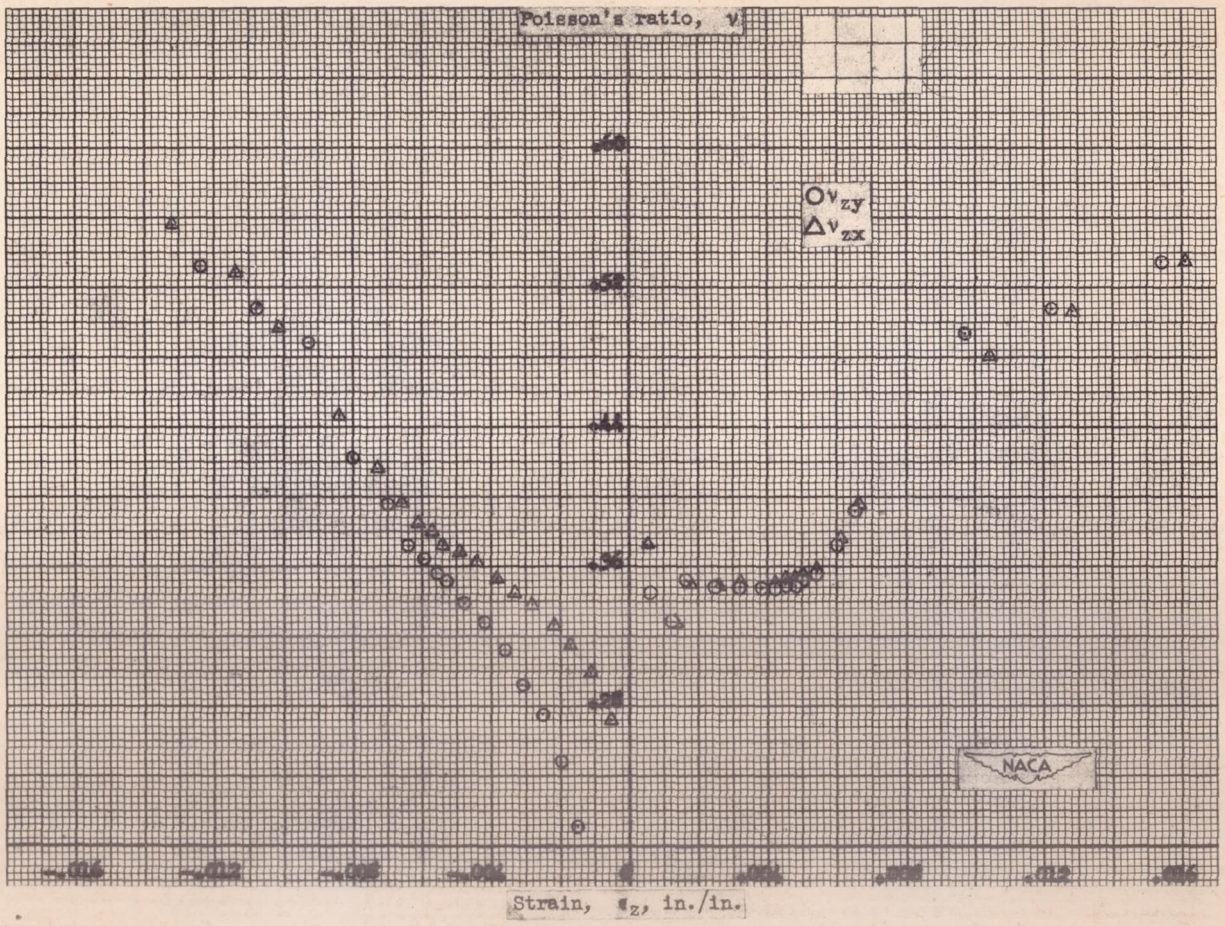

Figure 7.- Poisson's ratio variation for 14S-T6 aluminum alloy loaded in z-direction.

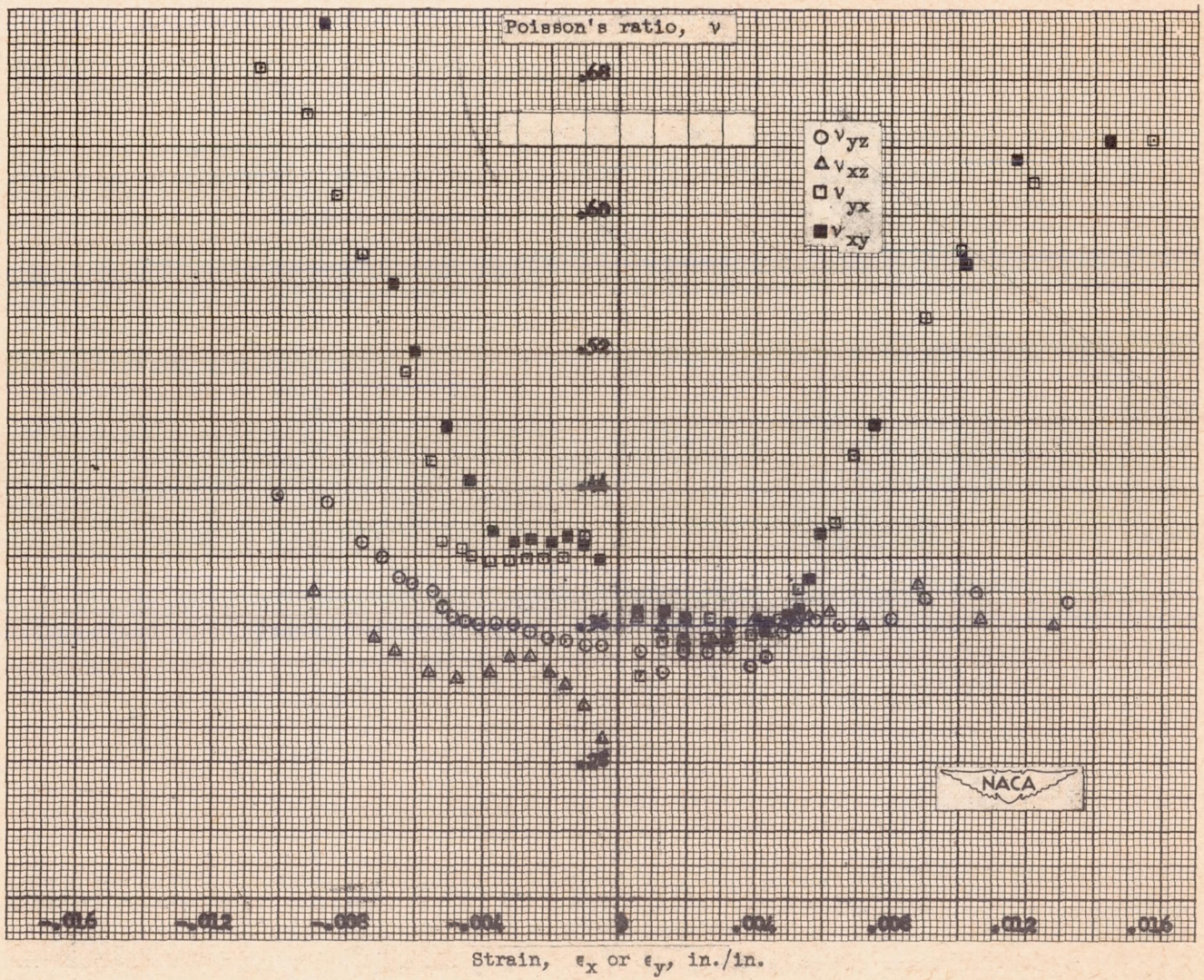

Figure 8.- Poisson's ratio variation for 14S-T6 aluminum alloy loaded in x- or y-direction.

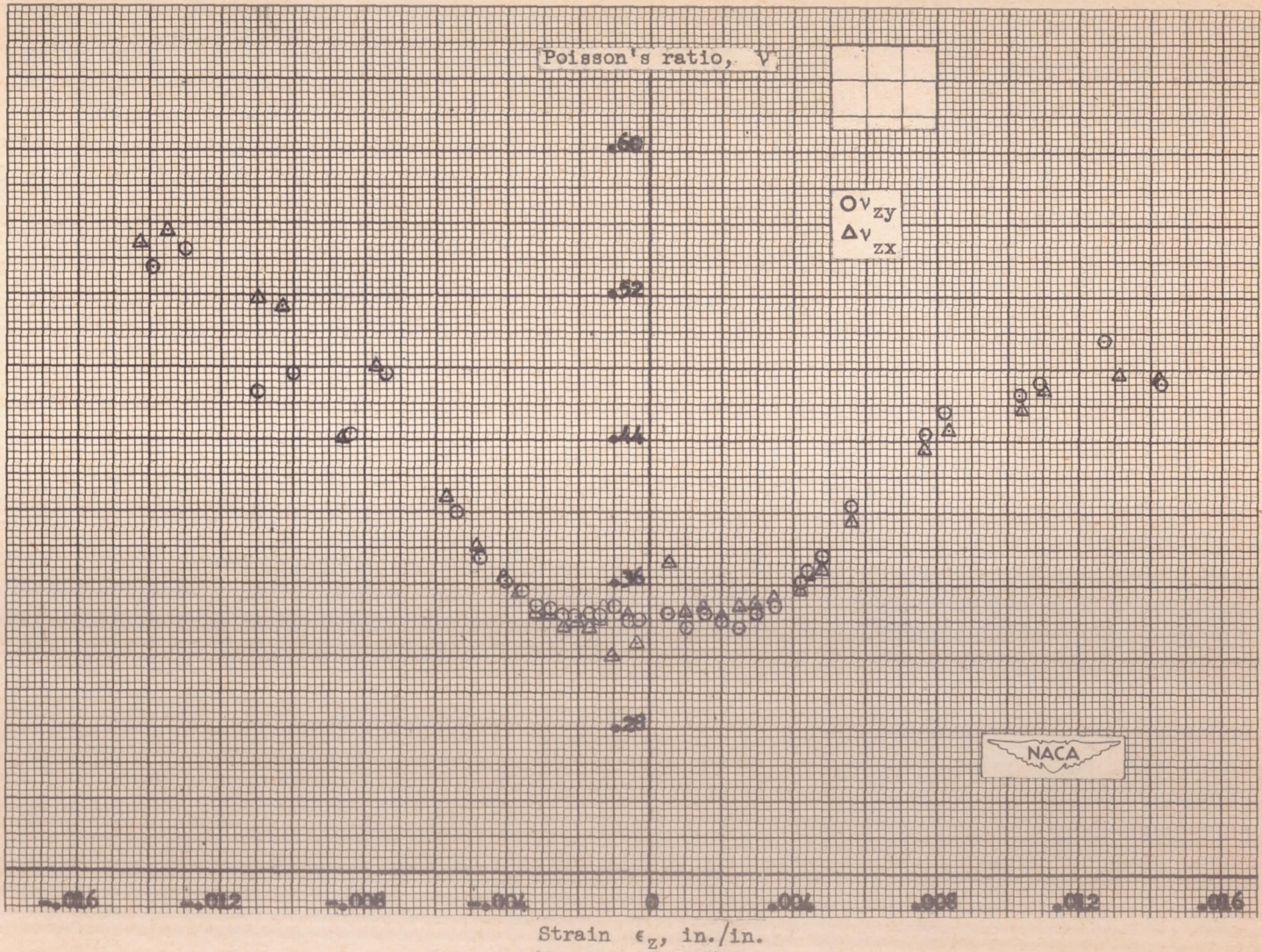

Figure 9.- Poisson's ratio variation for 24S-T4 aluminum alloy loaded in z-direction.

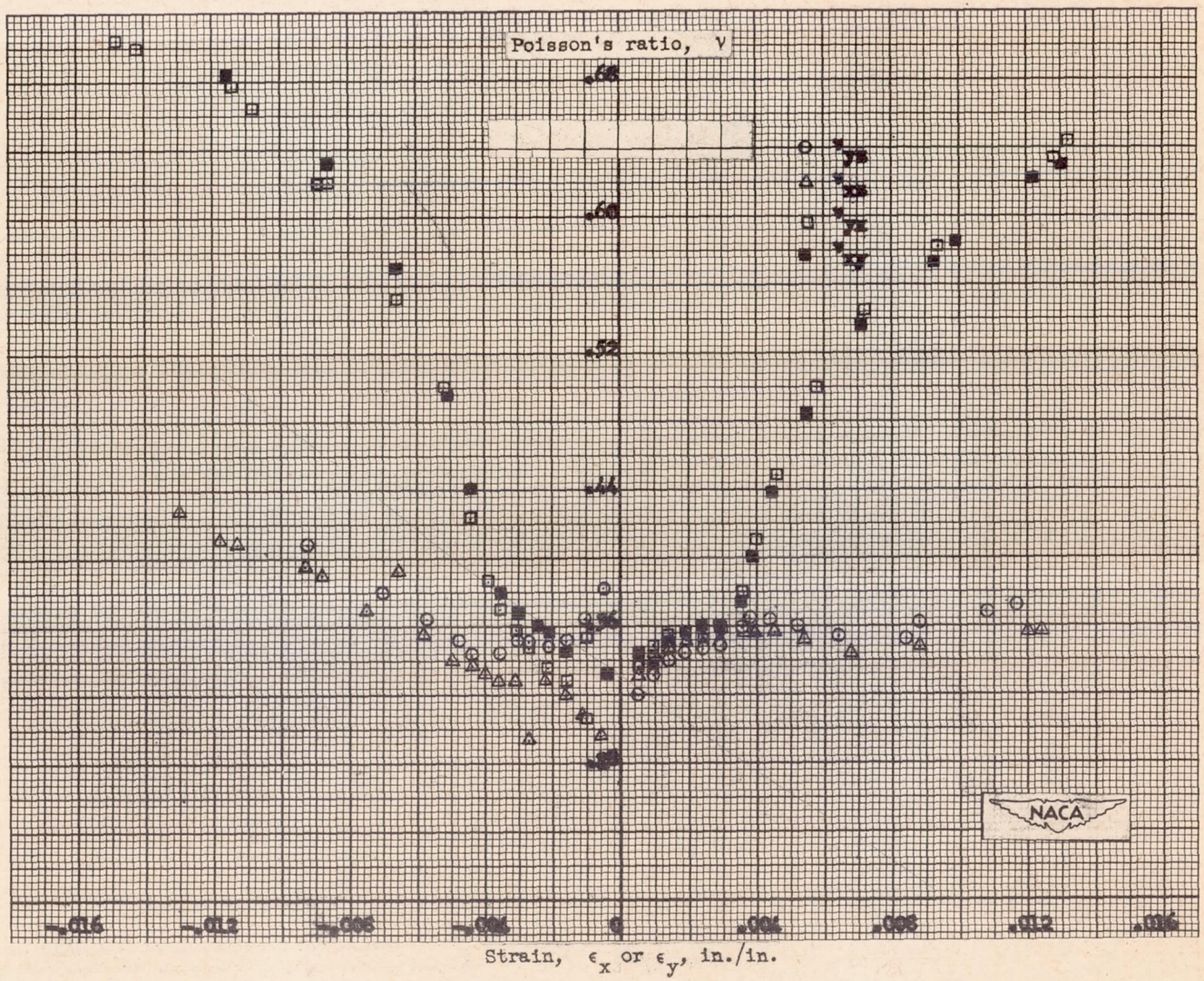

Figure 10.- Poisson's ratio variation for 24S-T4 aluminum alloy loaded in x- or y-direction.

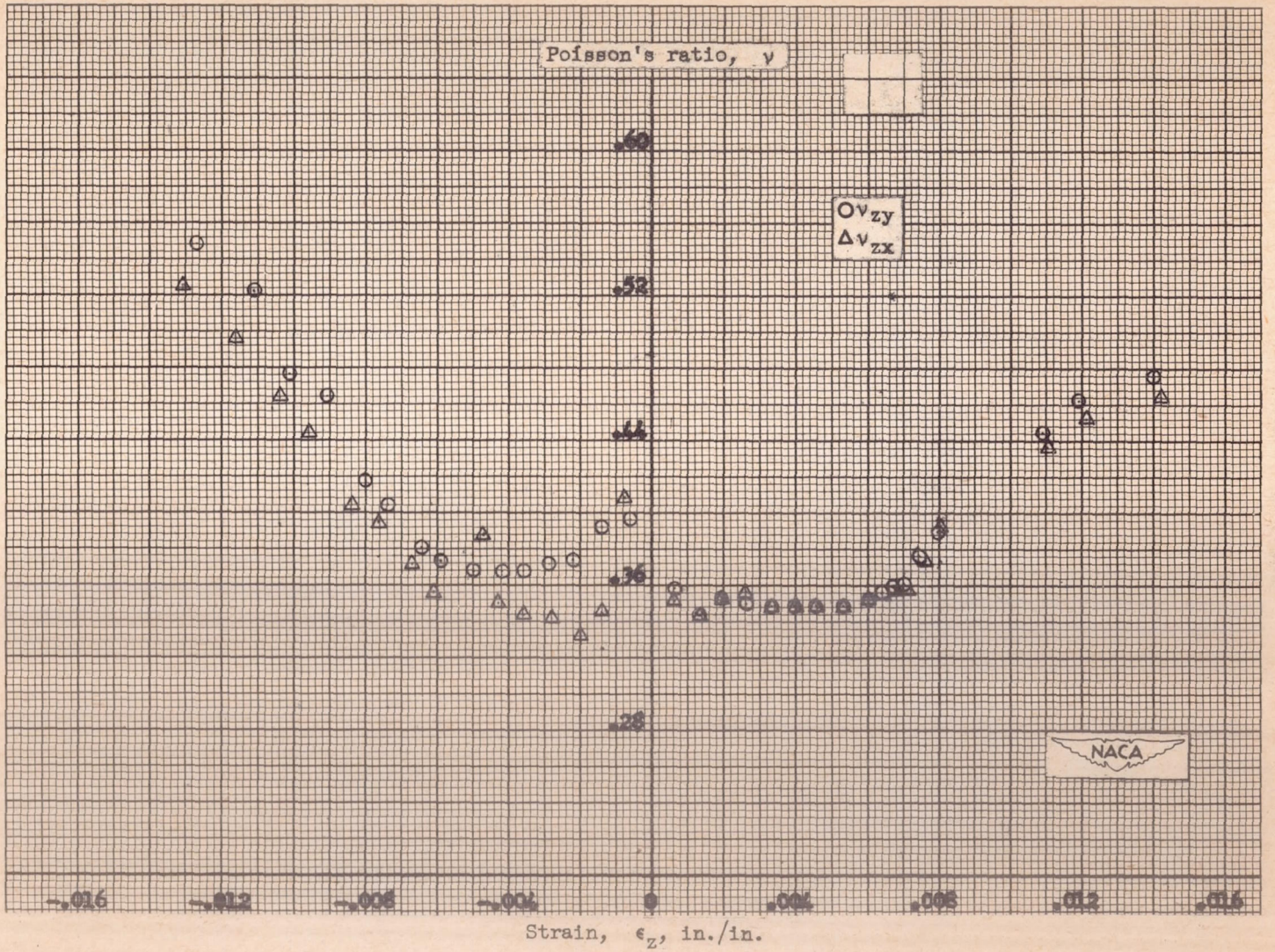

Figure 11.- Poisson's ratio variation for 75S-T6 aluminum alloy loaded in z-direction.

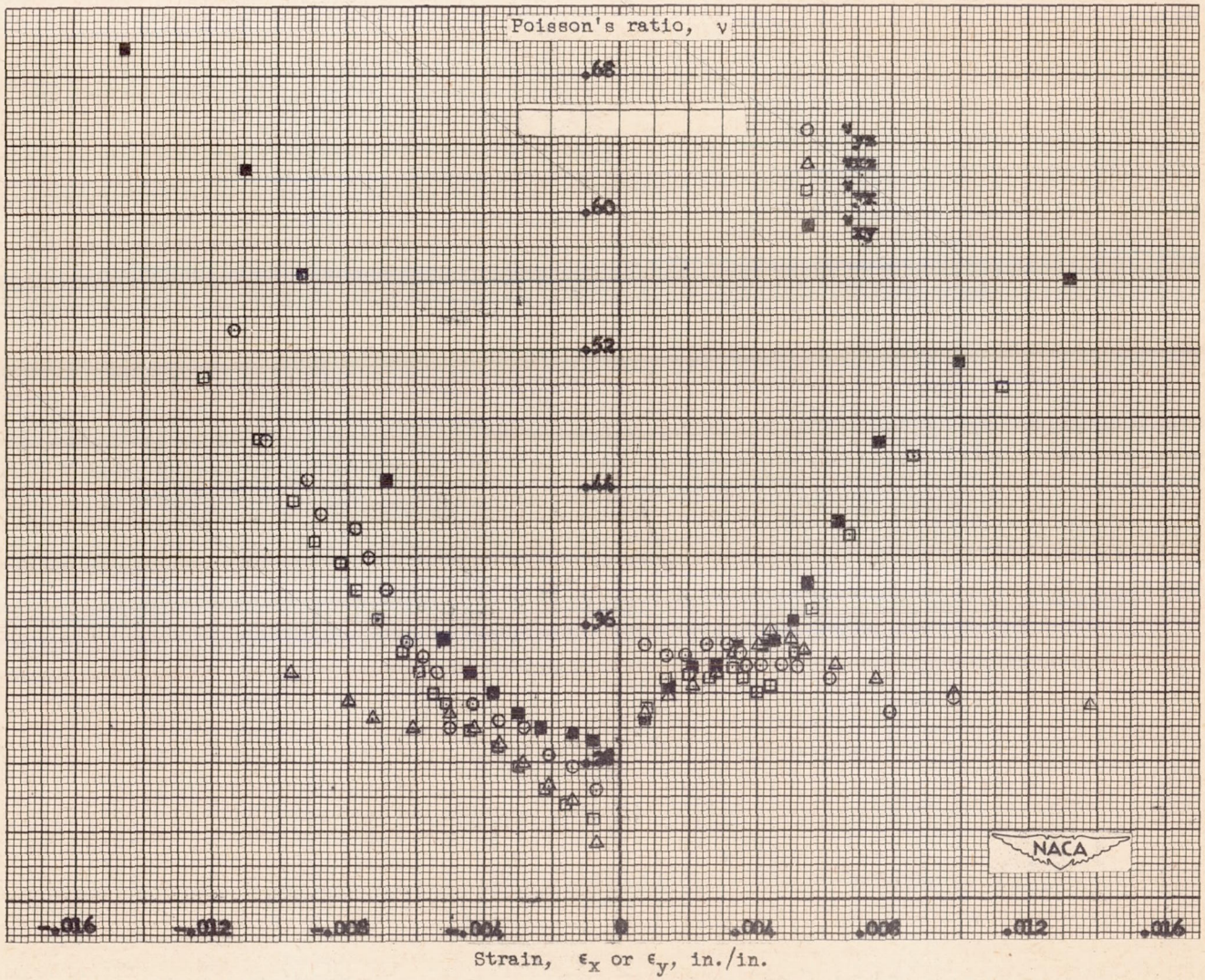

Figure 12.- Poisson's ratio variation for 75S-T6 aluminum alloy loaded in x- or y-direction.

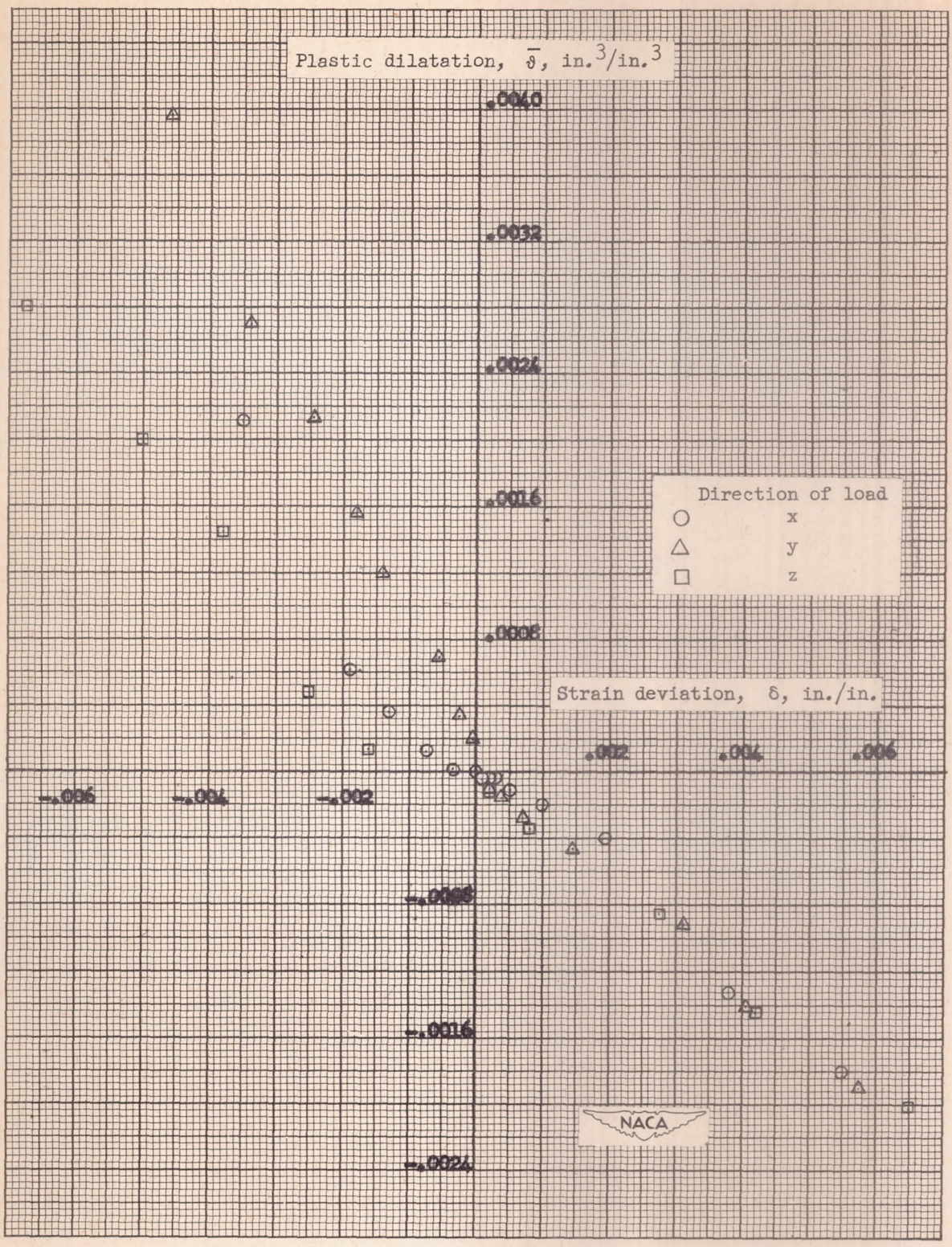

Figure 13.- Plastic dilatation against strain deviation for 14S-T6 aluminum alloy.

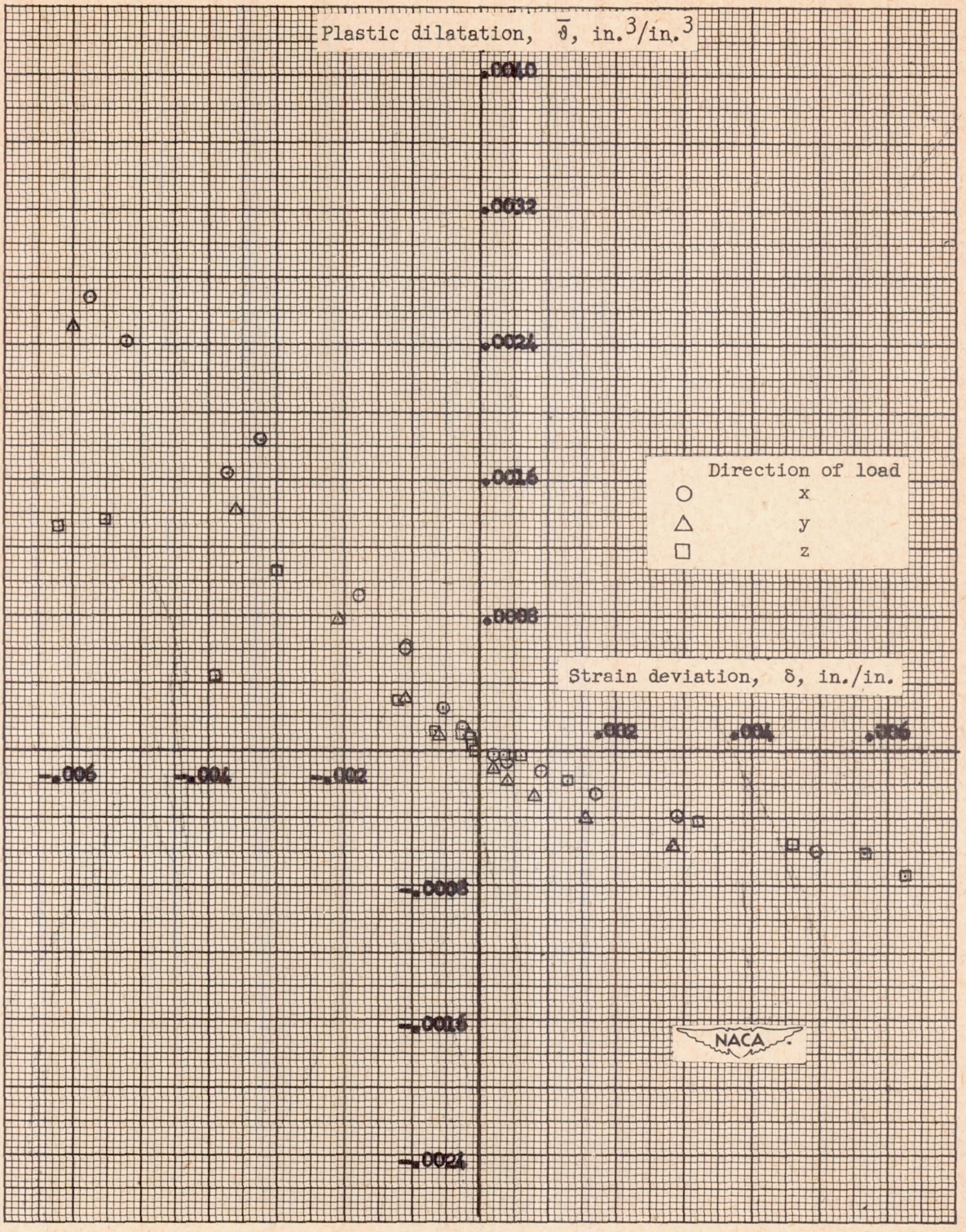

Figure 14.- Plastic dilatation against strain deviation for 24S-T4 aluminum alloy.

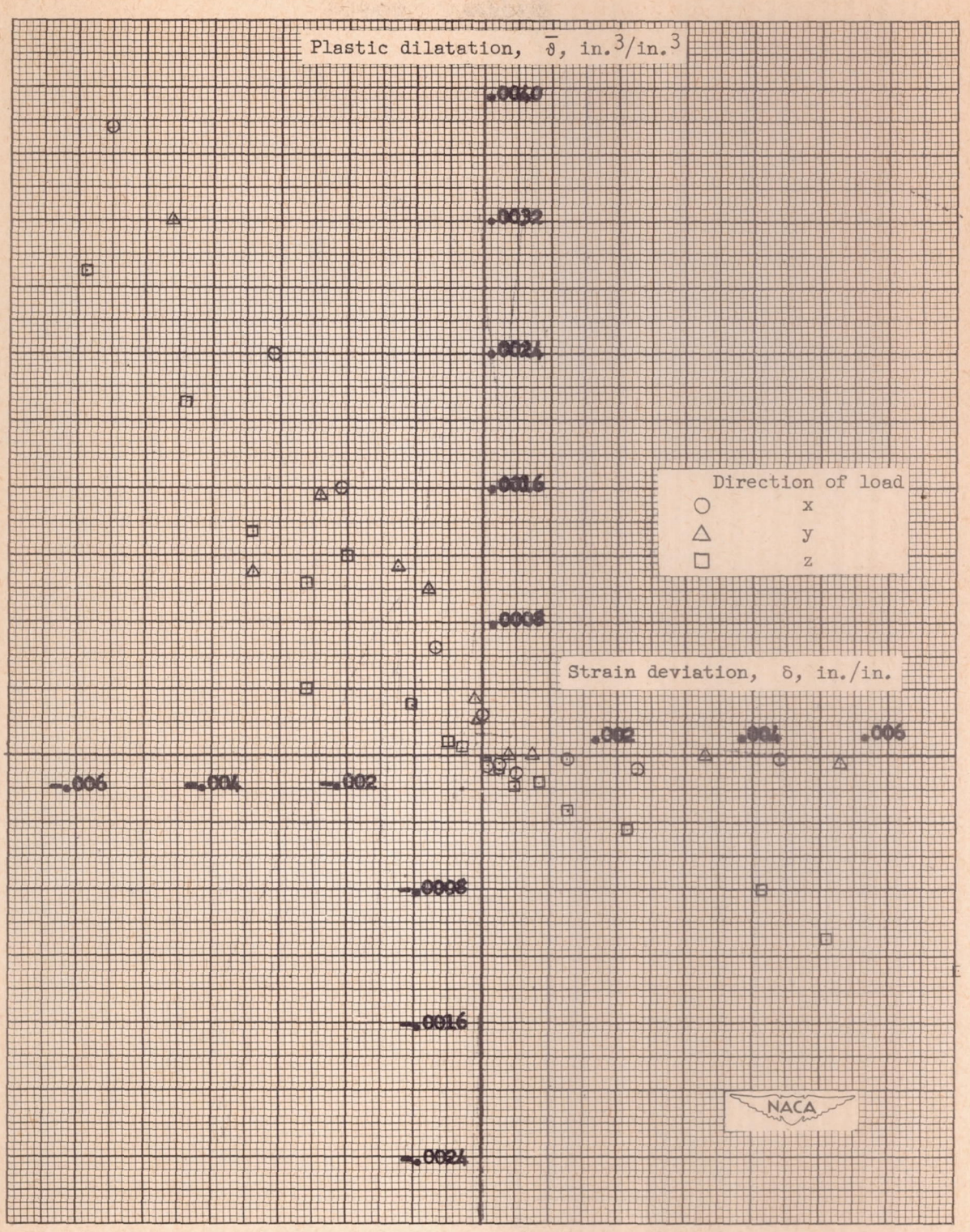

Figure 15.- Plastic dilatation against strain deviation for 75S-T6 aluminum alloy.

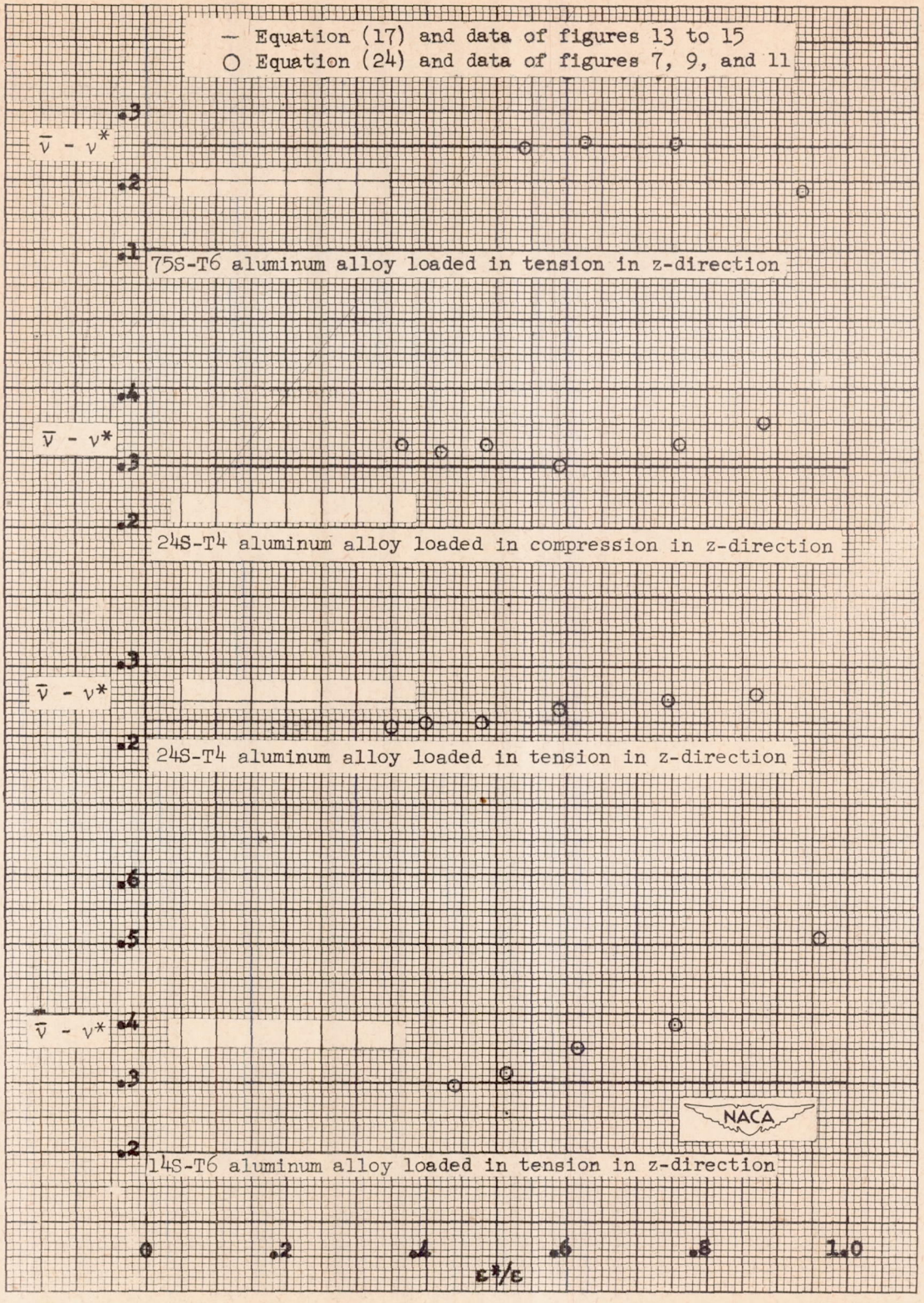

Figure 16.- Comparison of computed values of $\bar{\nu} - \nu^*$.